Ionics (2022) 28:767–777
https://doi.org/10.1007/s11581-021-04351-z

ORIGINAL PAPER

Electrochemical improvement in high-voltage Li-ion batteries by electrospinning a small amount of nano-Al_2O_3 in P(MVE-MA)/P(VdF-HFP)-blended gel electrolyte

Guojing Zang[1] · Min He[1] · Youhao Liao[1,2] · Minsui Li[1] · Mingyao Hong[1] · Weishan Li[1,2]

Received: 21 May 2021 / Revised: 23 September 2021 / Accepted: 24 October 2021 / Published online: 6 November 2021

Abstract

To improve the comprehensive performance of fibrous membrane based on poly(methyl vinyl ether-alt-maleic anhydride) P(MVE-MA)- and poly(vinylidene fluoride-co-hexafluoropropylene) P(VdF-HFP)-blended copolymers, a small amount of nano-Al_2O_3 was doped by electrospinning technique to apply for high-energy-density cathode material of nickel-rich $LiNi_{0.8}Co_{0.15}Al_{0.05}O_2$ (NCA) based Li-ion battery. The results indicated that the electrospinning membrane and corresponding gel polymer electrolyte (GPE) only doped with 3.0 wt.% nano-Al_2O_3 presented the proper structure and delivered the best electrochemical characterization. Due to the uniform distribution of nanoparticles on the fibers with higher density, the specific surface area and porosity of the fiber membrane were increased, leading to the improved fracture stress of 172.0 MPa for the membrane and ionic conductivity of 2.1×10^{-3} S cm^{-1} for the GPE at room temperature. Contributed from the proper pore structure and the enhanced interfacial stability, the capacity retention of 89.4% was achieved for the Li/GPE/NCA coin cell after 200 cycles in the voltage range of 3.0 V and 4.3 V under room temperature using the GPE doped with 3 wt.% Al_2O_3, compared with that of 63.6% for the GPE without nanoparticles. Similarly, the discharge capacity of the coin cell under 7*C* rate (123.2 mAh g^{-1}) maintained 65% of that at 0.3*C* (189.4 mAh g^{-1}), showing good rate performance of the developed GPE. Therefore, the significant improvement in electrochemical stability of the GPE achieved by doping a small number of nanoparticles provided a simple and feasible solution for the development of high-energy-density Li-ion batteries.

Keywords Lithium ion batteries · Gel polymer electrolyte · Nano-Al_2O_3 doped · Ceramic membrane · Electrospinning technique

Introduction

As a practical power and energy storage devices, secondary rechargeable lithium ion batteries (LIBs) have been widely used in different fields, ranging from small 3C electronic products to large-scale electric vehicles, and even energy storage base stations. Thus, LIBs show bright market prospects and development spaces, mainly caused by its relatively high energy density, long cycle life and environmental friendliness [1–3]. Generally, the cathode and anode in LIBs is physically isolated by separator, activating by the liquid electrolyte. However, the safety issue is followed along with the successful application of LIBs. Usually, the external factors that cause the unsafety of LIBs, such as abuse in the forms of over-charging, over-discharging, squeezing, and impacting, can be greatly avoided by standardizing the use of batteries. But the internal component of LIBs, for example, the application of low flash point and flammable carbonated liquid electrolyte, brings a great safety hazard to the battery in the case of thermal runaway [4]. Although the solid electrolytes of polymer or/and inorganic state without any liquid solvent can satisfy the safety requirements of LIBs, the room temperature ionic conductivity and the interfacial compatibility between solid electrolyte and electrode still need to be improved for the practical application of LIBs [5–8].

✉ Youhao Liao
liaoyh@scnu.edu.cn

[1] School of Chemistry, South China Normal University, Guangzhou 510006, China

[2] National and Local Joint Engineering Research Center of MPTES in High Energy and Safety LIBs, Engineering Research Center of MTEES (Ministry of Education), and Key Lab. of ETESPG(GHEI), South China Normal University, Guangzhou 510006, China

After decades of development, only the pursuit of higher energy density of LIBs can meet the different levels of requirements. To accomplish this goal, the applied cathode material should have higher operating potential and specific capacity, while the anode should possess the characterization of lower working potential and higher capacity. Among the reported cathode, the nickel-rich ternary cathode material of $LiNi_{0.8}Co_{0.15}Al_{0.05}O_2$ (LNCA) qualifies the requirements of high energy density, which turns into the exclusive cathode material for Tesla electric vehicle. Unfortunately, the matched carbonate liquid electrolyte tends to decompose when the operating voltage surpasses 4.2 V (vs. Li/Li^+). Thus, choosing a suitable electrolyte system matched LNCA cathode has become an intractable problem that must be solved in the development of high energy density battery.

In order to reduce or even eliminate the safety risks caused by the use of carbonated liquid electrolyte, the gel polymer electrolyte (GPE) is considered as the best alternative, since the GPE significantly reduces the activity of the liquid electrolyte by forming a gel state through adsorbing and swelling the removable liquid electrolyte into the polymer matrix. Furthermore, additional energy is required to separate the liquid electrolyte from the GPE compared with that directly from the liquid state electrolyte, which becomes much difficult to oxidize the liquid electrolyte in GPE. Thus, the improved oxidation stability of GPE is expected to match the high-voltage nickel-rich cathode. In addition, due to the flexibility and convenience in size, the GPE can be widely used in various fields during the design and assembly of the battery [9–11].

To a great degree, the properties of polymer matrix determine the performance of GPE. The first polymer used in GPE is polyethylene oxide (PEO), which is reported in 1973 by Wright et al. [12]. After that, poly(methyl methacrylate) (PMMA), poly(acrylonitrile) (PAN), polyimide (PI), and poly(vinylidene fluoride) (PVdF) polymerized by single monomer are fully investigated in the polymer LIBs [13–16]. Aiming at compensating for the weaknesses of a single polymer, copolymerization or blending of other functional monomers or polymers can significantly improve the comprehensive performance of GPE [17]. For example, the successfully used poly(vinylidene fluoride-*co*-hexafluoropropylene) P(VdF-HFP) copolymer with high ionic conductivity in commercial polymer LIB by Bellcore technique is formed through introducing amorphous HFP into highly crystalline PVdF oligomer [18]. The crystallinity of PVdF is greatly reduced due to the high elasticity of HFP segments in the polymer chain [19, 20].

Although the widely used P(VdF-HFP)-based GPE shows commendable film-forming properties, the lithium ionic conductivity and interfacial compatibility with electrode at high temperatures are still needed to be further modified by functional copolymer or inorganic particles for high-voltage LIBs [21]. According to our previous report [22], blending the secondary copolymer, methyl vinyl ether-maleic acid glycoside (P(MVE-MA)), significantly improves the rate performance of original P(VdF-HFP)-based GPE. However, the compatibility between the blended GPE and the nickel-rich ternary cathode material did not investigate. Furthermore, the higher ionic conductivity of GPE is required in order to improve the cyclic and rate capability of nickel-rich LIBs, which can be easily accompanied by doping inorganic nanoparticles. According to the Lewis acid-base theory, acidic nanoparticles have empty *d* orbitals in cations. Lone pair electrons in the anion from lithium salts (such as PF_6^-, ClO_4^-) can enter the empty orbitals of cations, making more free Li^+ dissociate from lithium salts, leading to the improvement in the ionic conductivity and the lithium ion transference number of bulk phase in GPE. Then, the most inorganic nanoparticles are atomic crystals with strong rigidity and high melting point, which can expect to effectively improve the mechanical strength and thermal stability of the developed membrane [23]. Additionally, nanoparticle shows superior electrophilic ability, which helps to maintain the good contact with the interface of electrode, resulting in the enhancement in the compatibility between GPE and electrode [13, 14].

Commonly, the nanoparticles used in GPE, such as Al_2O_3, SiO_2, and TiO_2, play a crucial role in the ionic conductivity and the interfacial stability of the GPE [24–29]. However, the lowest weight content of nanoparticle in the reported GPE is usually as high as 10 wt.% [30–37]. To reduce the manufacturing cost, a small amounts of nano-Al_2O_3 is doped in the P(MVE-MA)-P(VdF-HFP) fiber membranes through the electrospinning technology in this investigation. The performances of membranes and corresponding GPEs are studied by the physical and electrochemical characterization. By analyzing the effect of nanoparticle doping ratio on the performances of GPEs, the optimal mass ratio of only 3% Al_2O_3 significantly enhances the mechanical strength and electrochemical stability of GPE, which is expected to be applied in the high-energy-density LIBs.

Experimental

Preparation

Poly(vinylidene fluoride-*co*-hexafluoropropylene) (P(VdF-HFP)) (M_w = 400,000, Sigma − Aldrich), poly(methyl vinyl ether-*alt*-maleic anhydride) (P(MVE-MA) (M_w = 216,000, Aladdin), and nano-Al_2O_3 (average particle size of 30 nm, Aladdin) were used as purchased. To obtain the nanoparticles contained copolymer slurry, the mixed solvents of acetone and N,N-dimethylacetamide (DMAC) with mass ratio of 7:3 were firstly added into a three-necked flask. After

that, the different mass ratios of nano-Al_2O_3 (0 wt.%, 1.5 wt.%, 3.0 wt.%, and 4.5 wt.%, based on the total weights of polymers) were added, respectively. The flask was sonicated for 1 h in the ultrasonic machine. After the nanoparticles were evenly dispersed into the mixed solvent, the blended polymers with the mass ratios of P(MVE-MA):P(VdF-HFP) = 3:1 were added into the flask based on our previous work [22]. The mixtures were mechanically stirred at a speed of 300 r min^{-1} for 2 h at 60℃ to obtain homogeneous slurry with the solid content of 16%.

The slurry was transferred into the 1 mL capillary syringe pump in electrospinning machine (SS series, Ucalery, China). In order to improve the mechanical strength of the membrane, polyethylene (PE) was selected as a support. The fibers were collected on both sides of PE separator under the specific electrospinning conditions (humidity: 35%, electric field intensity: 18 kV, flow velocity: 1 mm min^{-1}, receiving distance: 20 cm, translational distance: 100 cm) at room temperature [38]. The electrospinning membranes with different contents of nano-Al_2O_3 were transferred to a vacuum oven at 40℃ and dried for 12 h to fully evaporate the solvent. The thickness of the obtained membrane was 40−45 μm.

To prepare the corresponding gel polymer electrolyte (GPE), the membranes were placed in 1 mol L^{-1} $LiPF_6$ liquid electrolyte consisting of the carbonate solvents of ethylene carbonate (EC), dimethyl carbonate (DMC) and ethyl methyl carbonate (EMC) in the volume of 3:2:5 (Dongguan Kaixin Electrolyte Co. Ltd., battery grade) for 0.5 h in argon-filled glove box, where the contents of oxygen and water was controlled below 0.1 ppm. The active material of $LiNi_{0.8}Co_{0.15}Al_{0.05}O_2$ (NCA, Guangzhou Tianci High-tech Materials Co. Ltd.), conductive agent of carbon black, and PVdF binder (Shenzhen Kejing Zhida Technology Co. Ltd.) with the mass ratio of 8:1:1 were dissolved in N-methylpyrrolidone (NMP) solvent to obtain a viscous slurry. The NCA electrode was obtained by coating the slurry onto the aluminum foil using a scraper, transferring to a vacuum oven for drying, and rolling orderly. A series of CR2025 type coin cells with the structures of SS (stainless steel)/GPE/SS, Li/GPE/Li, and NCA/GPE/Li were assembled in the glove box for the sake of testing the electrochemical performance of the nanoparticle-doped membranes and GPEs.

Characterizations

The scanning electron microscope (SEM, JEOL, JSM − 6510A, Japan) at an acceleration voltage of 15 kV was used to survey the surface morphology of the nano-Al_2O_3-doped fiber membranes. The fracture stress in the form of mechanical strengths for the electrospinning membranes were tested through a tensile strength instrument (XLW − EC, Labthink, China). The bulk resistance (R) of GPE at room temperature was gained by electrochemical impedance spectroscopy (EIS) (PGSTAT − 30, Autolab Metrohm, the Netherlands) using the sandwiched SS/GPE/SS coin cell. The applied potential amplitude was 5 mV while the frequencies was from 500 kHz to 1 Hz. The ionic conductivity (σ) was calculated from Eq. (1):

$$\sigma = l/RS \tag{1}$$

where l was the thickness of GPE and S was the contact area between GPE and SS disk (contacted diameter: 14 mm). The R value was the intersection of the line constituted by Nyquist plot and the abscissa axis.

The lithium ion transference number (t_+) reflected the carrier migration properties of LIBs, which was the ratio of the migration current caused by lithium ion to the total current. The smaller value of t_+ indicated the more serious polarization inside the battery. Although the ideal value of t_+ was one, the value in GPE was usually less than 0.5 caused by the interaction between solvent molecules and lithium ions [39]. The t_+ of nanoparticle-doped GPE was measured using steady-state dc polarization method by the combination of chronoamperometry (CA) and EIS measurement in the symmetrical coin cell with the structure of Li/GPE/Li [40, 41], whose value was obtained by Eq. (2).

$$t_+ = \frac{I_S(\Delta V - I_O R_O)}{I_O(\Delta V - I_S R_S)} \tag{2}$$

where ΔV was the applied potential with the value of 10 mV during potentiostatic polarization in CA measurement in this work, I_0 and I_S were the values of initial and steady-state current in the chronoamperometry curve, while R_0 and R_S were the resistances before and after CA polarization from EIS measurement, respectively.

The interfacial compatibility of GPE with lithium anode was understood by the change of resistance along with the storage time using the cell of Li/GPE/Li, which was tested by EIS with potential amplitude of 5 mV and the frequencies from 500 kHz to 0.03 Hz. In order to evaluate the cycle stability and rate capacity of the prepared GPEs at ambient temperature, the coin cell of Li/GPE/NCA was tested under different rates on the Land Battery Test System (Land CT2001A, Wuhan, China).

Results and discussion

SEM images of the prepared membranes

The structure of the prepared membrane plays a key role in electrochemical stability of the corresponding battery, which can be visually observed by SEM. Figure 1 shows the SEM images of P(MVE-MA)-P(VdF-HFP)-Al_2O_3/PE-based fiber membranes with different proportions of nano-Al_2O_3. As

can be observed from a low magnification image, there is no significant distinction in the overall appearance of the membranes, which shows cross-linked structure with uniform pores among the similar diameters of fibers. However, under a high magnification field of vision in the embedded figures, it is found that the surface of the fiber undergoes significant changes. With the increased proportion of nanoparticles, the inlaid amount of nanoparticles on the surface of the polymer fibers are also aggrandized gradually. The surface of fibers without nanoparticles is rough. After doping 1.5 wt.% nano-Al_2O_3 in polymer fiber, the surface scattered with a small number of nanoparticles becomes relatively smooth. Increasing the doped contents of nano-Al_2O_3 in polymer, the embedding amount of nanoparticles is enhanced significantly along with the uniform distribution. Especially for the membrane incorporated with 3.0 wt.% nano-Al_2O_3 in Fig. 1c, the fiber diameter and the formed pore size should be the most suitable for electrochemical performance of corresponding assembled battery. Further increasing the content of nano-Al_2O_3 to 4.5 wt.%, not only the fabrication cost of membrane is elevated, but also the nanoparticles are prone to agglomerate to form micron level secondary particles in Fig. 1d, resulting in the reduction of the cross-linking degree for the membrane, which is harmful for the mechanical strength and electrochemical characterization of GPE.

Mechanical strength of membrane

The dual functions of the GPE in LIBs can be ascribed to block the electrons to prevent direct contact between cathode and anode, and fast transports lithium ions simultaneously. The implementation of these functions for the developed membranes mainly depends on the performances of mechanical strength and ionic conductivity. Super mechanical strength can ensure that of the membrane will not be punctured or broken during the assembly process, and prevent the short circuit inside the battery. Figure 2 presents the relationship between elongation rate and stress at break for the membranes with different mass fractions of nanoparticles. The fracture stress of the doped membranes with the contents of 0 wt.%, 1.5 wt.%, 3.0 wt.%, and 4.5 wt.% are 139.4 MPa, 172.0 MPa, 177.1 MPa, and 170.0 MPa, while the corresponding elongations at break are 121%, 133%, 97%, and 88%, respectively. The results indicate that doping nano-Al_2O_3 in the membrane increases the rigidity and tensile strength of the membrane to a certain extent, attributed from the rigidity of nano-Al_2O_3. Meanwhile, the doping amount of nanoparticles affects the mechanical strength of

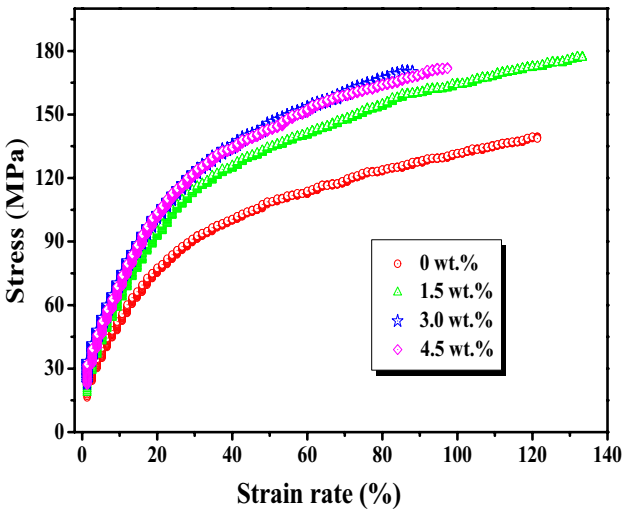

Fig. 2 Stress–strain curves for the blended membranes doped with different contents of nano-Al_2O_3

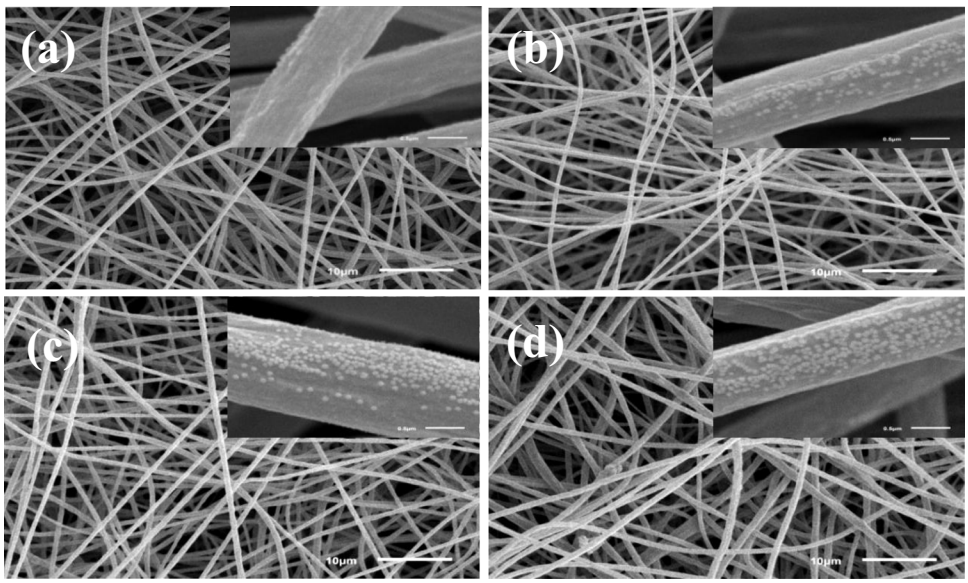

Fig. 1 SEM images for the electrospinning fibrous membranes blended with different mass ratio of nano-Al_2O_3: **a** 0 wt.%, **b** 1.5 wt.%, **c** 3.0 wt.%, and **d** 4.5 wt.%

the membrane: lower added amount of nanoparticles contributes to the flexibility, while higher-doped content goes against due to the high coverage of nanoparticles on the fiber surface. Thus, the nanoparticle content of 3.0 wt.% should be the suitable proportion for the mechanical strength of membrane, which is selected for the next investigation combined with SEM observation.

Ionic conductivity of GPE

The lithium ionic conductivity of the GPE (gel polymer electrolyte) reflects the ability to carry the current through the movement of lithium ions in the bulk electrolyte. Figure 3 presents the Nyquist plots of GPEs doped with different proportions of nano-Al_2O_3 at room temperature. Compared with the GPE without nanoparticles, the impedance of lithium ions in nano-Al_2O_3-doped GPE becomes smaller. The calculated value from Eq. (1) is 1.3×10^{-3} S cm^{-1} for the GPE without Al_2O_3, which meets the application requirements in LIBs. After doping, the ionic conductivity becomes 2.1×10^{-3} S cm^{-1} when the mass fraction of nano-Al_2O_3 is 3.0 wt.%, which is slightly higher than that of 1.5 wt.% (1.5×10^{-3} S cm^{-1}) and 4.5 wt.% (1.6×10^{-3} S cm^{-1}). Therefore, doping small amount of nanoparticles in polymer membrane should be an effective way to improve the ionic conductivity of GPE.

Based on Lewis acid-base theory, Al_2O_3 belongs to Lewis acid since it can accept electronic pairs by the empty 3d orbit in Al^{3+}. During ions transportation, PF_6^- anion cluster dissociated from lithium salt $LiPF_6$ will easily enter the empty orbit of Al_2O_3. To compensate for the loss of anions, more lithium ions are dissociated, which contributes to increase the concentration of lithium ions in the bulk electrolyte and improve the lithium ionic conductivity in GPE system subsequently. However, caused by the natural agglomeration of

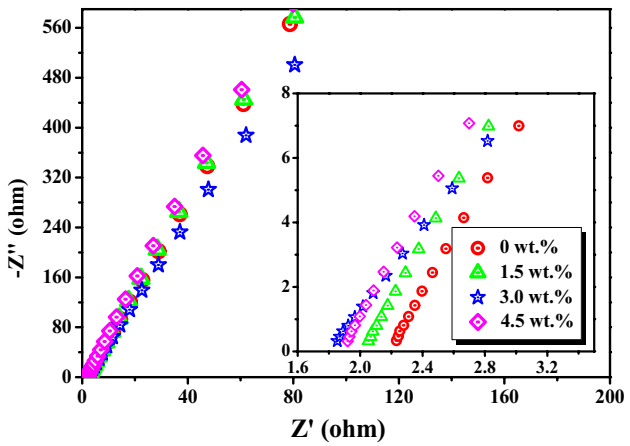

Fig. 3 Nyquist plots for the block cell of SS/GPE/SS at room temperature using the GPE with different mass ratios of nano-Al_2O_3

nanoparticles, excess Al_2O_3 is easy to block the migration channel of lithium ions, resulting in a slight decrease in the ionic conductivity. According to the report, the lowest mass fraction of nano-Al_2O_3 in P(VdF-HFP)-based GPE system to achieve the highest ionic conductivity of 1.9×10^{-3} S cm^{-1} is 10 wt.% by liquid–liquid extraction process [42]. Interestingly, the added amount of nanoparticles reduces to 3.0 wt.% in P(MVE-MA)-P(VdF-HFP) based GPE due to the advanced electrospinning technique that helps to evenly disperse the nanoparticles into the polymer at this work, which should be the lowest amount in ceramic-doped membrane currently.

Lithium ion transference number of GPE

In order to further understand the transfer behavior of lithium ions, the electrospun GPEs are assembled into Li/GPE/Li symmetrical coin cell to obtain their lithium ion transference number (t_+) combined with AC impedance spectrum and DC-induced polarization methods. As shown in Fig. 4a, the impedance of GPE without nanoparticle increases from 47 to 58 Ω after applied a tinny potential of 10 mV, while the response current stabilizes from 360 to 67 μA; thus the calculated t_+ is 0.51. After doping 3.0 wt.% nanoparticle, the changed values of impedance and current is smaller, where the impedance increases from 31 to 34 Ω, and the current from 340 to 120 μA, leading to the enhancement in the t_+ of 0.61, which is also higher than that of 0.52 for GPE doped with 1.5 wt.% Al_2O_3 and that of 0.60 for GPE with 4.5 wt.% Al_2O_3. It seems that further increasing the amount of nanoparticle will not contribute to the transfer of lithium ions, which should be caused by that the agglomeration of secondary particles blocks the free diffusion of lithium ions in GPE from the increased interfacial transfer resistance. Interestingly, the calculated results of t_+ are in good agreement with the room temperature ionic conductivity, reconfirming that adding 3.0 wt.% Al_2O_3 in membrane is sufficient to make the GPE perform excellent transference ability for lithium ions, which should be beneficial to the cyclic and rate characterization of the assembled battery.

Interfacial compatibility of GPE with lithium anode

Compared with the commercial graphite anode with the specific capacity of 372 mAh g^{-1}, the lithium metal exhibits much higher theoretical capacity of 3860 mAh g^{-1}, which should be the most promising anode material for LIBs. Thus, the compatibility of the developed GPE with the lithium anode becomes specifically important for the electrochemical performance of the corresponding battery, which is obtained by monitoring the changes of impedance over the storage time using Li/GPE/Li type coin cell. As exhibited in Fig. 5, the diameter of the flattened semicircle composed

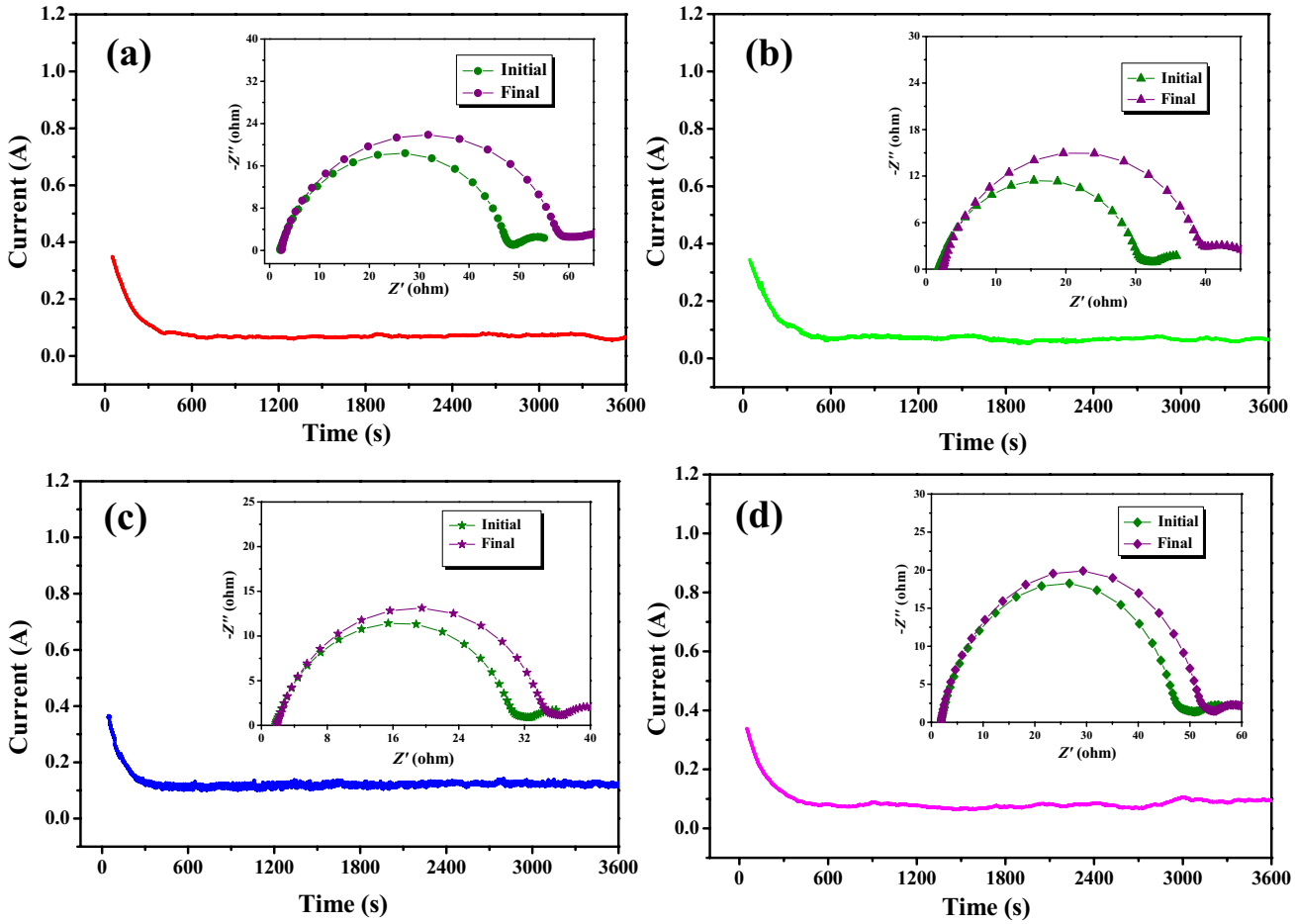

Fig. 4 Electrochemical impedance spectra and DC polarization curves for GPEs doped with various contents of Al_2O_3: **a** 0 wt.%, **b** 1.5 wt.%, **c** 3.0 wt.%, and **d** 4.5 wt.%

of the Nyquist plots is considered as the interfacial impedance, which is generated by the charge transfer resistance in the electrolyte/electrode interface. It can be found from Fig. 5a that the GPE without nanoparticle exhibits highest interfacial resistance of 56 Ω after setup, and increases to 67 Ω after 15 days of storage.

Doping Al_2O_3 in electrospinning membrane does reduce the interfacial resistance whether it is freshly assembled or has been stored for 15 days, caused by the improvement in the compatibility between the GPE and lithium anode. Especially for the GPE doped with 3.0 wt.% nanoparticles in Fig. 5c, the increased magnitude is from 32 to 35 Ω after 15 days of storage, indicating that proper amount of Al_2O_3 helps the polymer absorb the flowing liquid electrolyte to reduce its reaction activity, thereby inhibiting the reaction between the electrolyte and the lithium electrode and slowing down the growth rate of the passivation layer. In addition, resulted from that the nanoparticles with a large specific surface area can effectively absorb the impurities in GPE, such as a small amount of water, the side reactions of impure materials in contact with lithium metal have been prevented subsequently. Therefore, the reduced activity helps to stabilize the interface between the GPE and the electrode. However, further increasing the amount of Al_2O_3 nanoparticles in GPE, the effect is not obvious, ascribed from the partial agglomeration of nanoparticles. The superior compatibility of developed GPE with lithium anode suggests that the formed solid electrolyte interface (SEI) layer on the surface of lithium anode is well maintained, guaranteeing the long cycling stability of the full cell.

Electrochemical performance of GPE

The key parameter determined whether the nanoparticle-doped GPE can be used in actual production or not is the cycle and rate performance of the assembled battery. Thus, nickel-rich $LiNi_{0.8}Co_{0.15}Al_{0.05}O_2$ (NCA) is selected as cathode material and lithium metal as anode material to evaluate the electrochemical stability of the developed GPE by Li/GPE/NCA coin cell. Aiming at improving

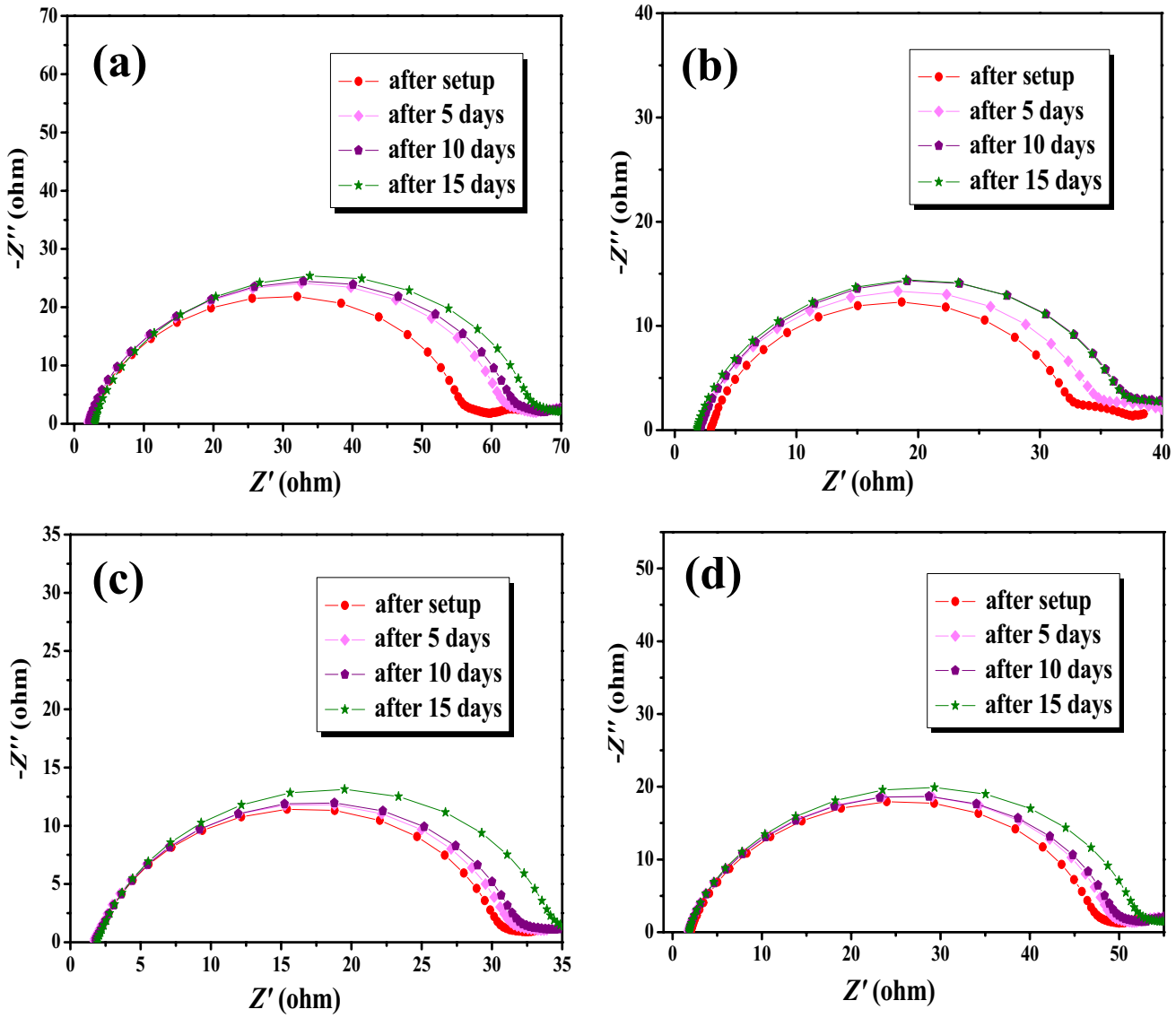

Fig. 5 Electrochemical impedance spectra as function of time for the Li/GPE/Li coin cells using the GPEs with **a** 0 wt.%, **b** 1.5 wt.%, **c** 3.0 wt.%, and **d** 4.5 wt.% nano-Al_2O_3

the energy density of battery, the fabricated coin cells are charged to high voltage of 4.3 V and discharged to 3.0 V at room temperature under 1*C* rate for the cyclic performance. As presented in Fig. 6, the retention ability of discharge capacity is only 63.6% after 150 cycles for the GPE without nanoparticles, which rapidly decays from 167.7 to 106.6 $mAhg^{-1}$. Interestingly, the cyclic stability of Al_2O_3-doped GPE is significantly improved, especially for the GPE with 3.0 wt.% nanoparticles, which retains 89.4% of initial capacity under the same test conditions (from 174.5 to 156 mAh g^{-1}).

During the long cycle of the battery, thermal shrinkage of the membrane from the delay of internal heat dissipation, the structural damage by the dissolution of the transition metal from the cathode material, and the decomposition of the electrolyte will gradually reduce the capacity of the battery. Due to the rigidity of inorganic ceramics, Al_2O_3-doped GPE can prevent thermal shrinkage during the cycle and provide smooth channels for the transference of lithium ion. At the same time, the gelation reaction of GPE reduces the activity of liquid electrolyte, which greatly decrease the decomposition of electrolyte itself and the reaction with the cathode material simultaneously, preventing the structure from being destroyed. Therefore, suitable ceramic particles contained GPE exhibits good cycle performance. However, when the content of nanoparticles in GPE increases to 4.5%, the pore structure of the membrane will be partially blocked due to the spontaneous agglomeration of nanoparticles, and the

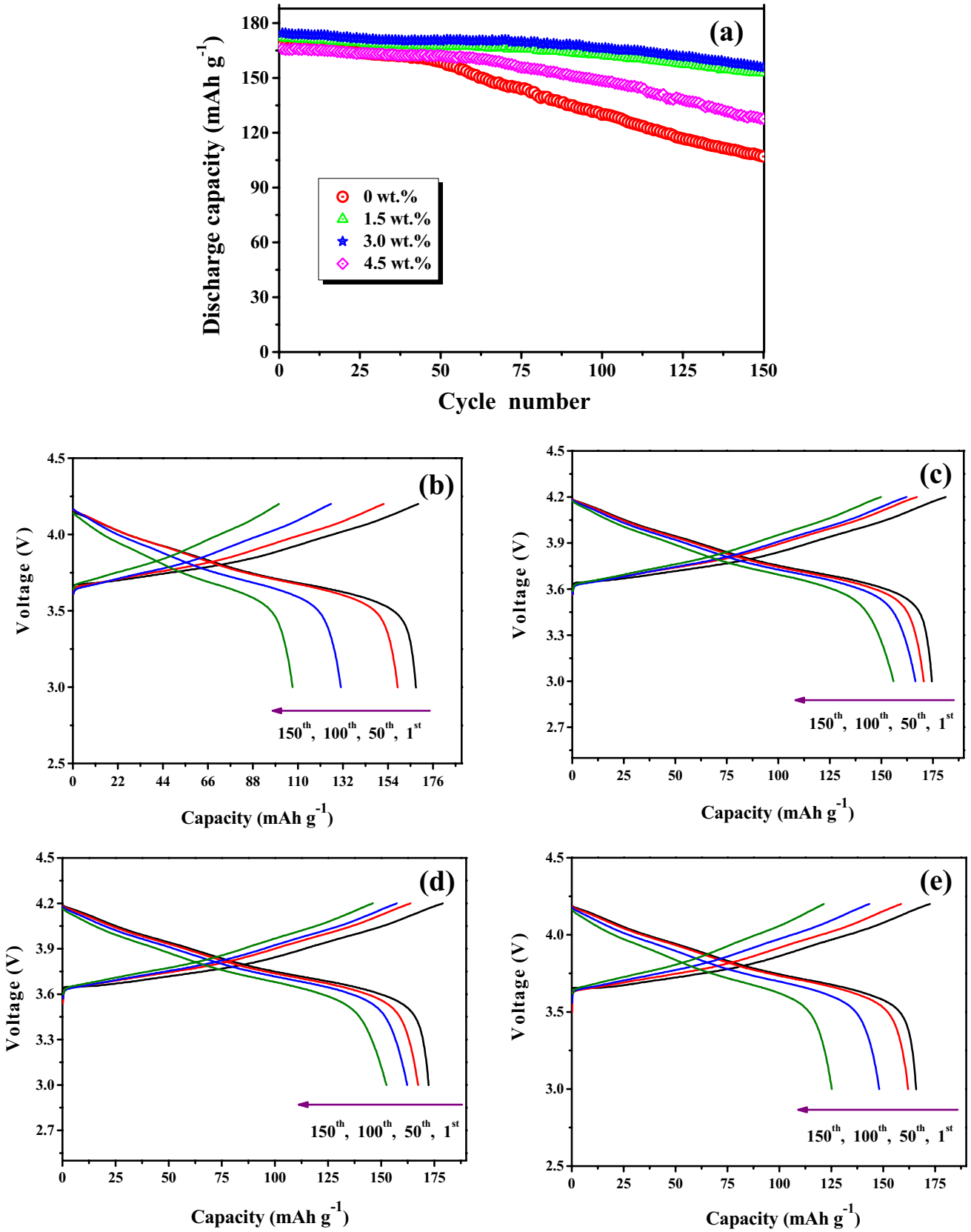

Fig. 6 **a** Cyclic stability of Li/GPE/$LiNi_{0.8}Co_{0.15}Al_{0.05}O_2$ coin cell under 1*C* rate in the voltage range of 3.0 V and 4.3 V at ambient temperature; the corresponding charge/discharge curves using **b** 0 wt.%, **c** 1.5 wt.%, **d** 3.0 wt.%, and **e** 4.5 wt.% nano-Al_2O_3 doped GPEs

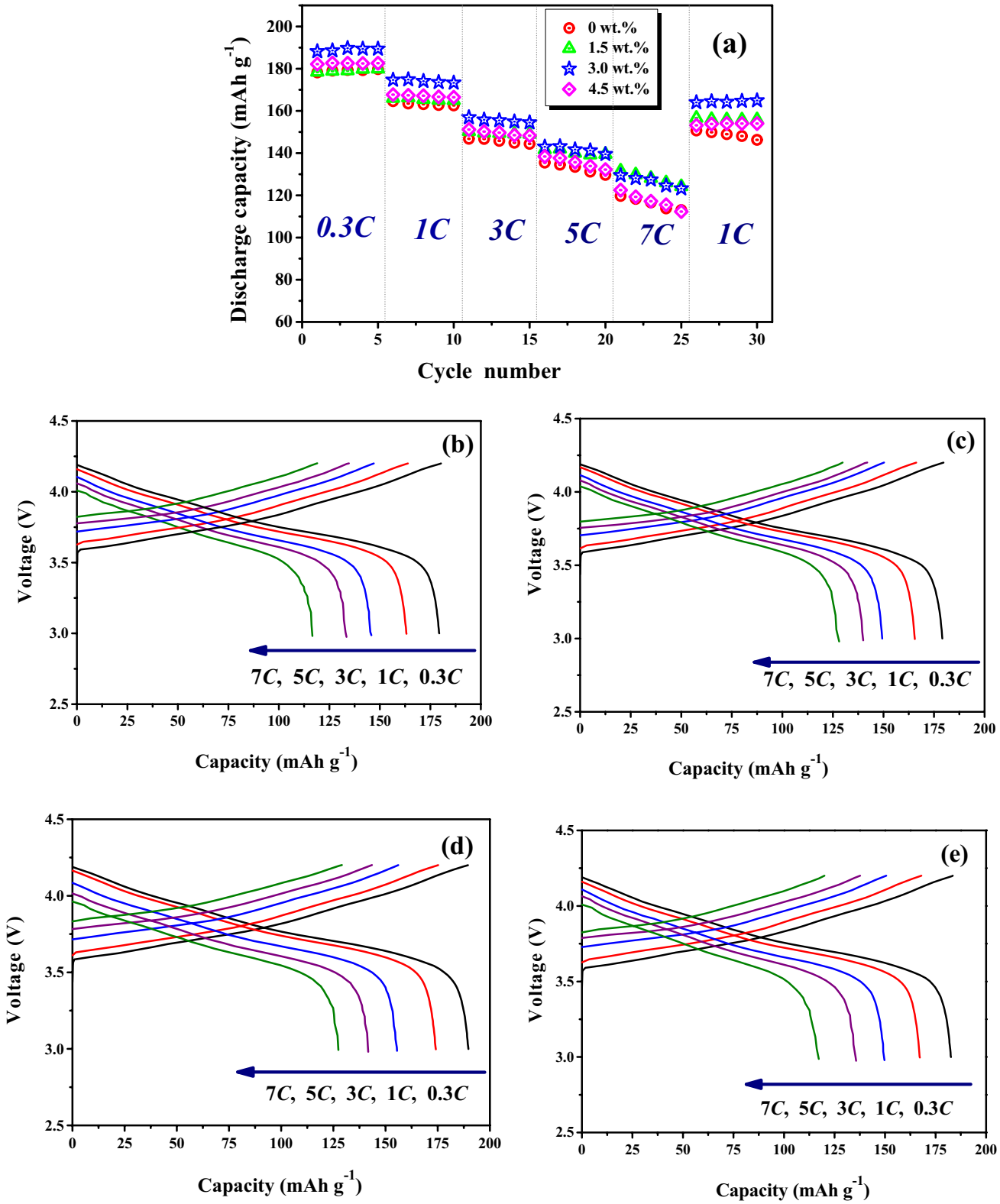

Fig. 7 **a** Rate capacity of Li/GPE/$LiNi_{0.8}Co_{0.15}Al_{0.05}O_2$ coin-cell in 3.0 V and 4.3 V at ambient temperature; the corresponding charge/discharge curves under the 3rd, 8th, 13th, 18th, and 23rd cycle using **b** 0 wt.%, **c** 1.5 wt.%, **d** 3.0 wt.%, and **e** 4.5 wt.% nano-Al_2O_3-doped GPEs

lithium ions cannot effectively diffuse to the other side of the polymer membrane, resulting in the inability of lithium ions to migrate quickly by the formation of partial concentration polarization, leading to slightly lowering the cycle stability of the battery.

Figure 7 presents the rate performance and the detail charge/discharge curves under the 3rd, 8th, 13th, 18th, and 23rd cycle for Li/GPE/NCA coin cell using the GPEs with different proportions of nano-Al_2O_3 at room temperature. All the coin cells are cycled for each 5 cycles at the rates ranging from 0.3*C*, 1*C*, 3*C*, 5*C*, 7*C* to 1*C* in voltage of 3−4.3 V. The discharge capacity is decreased along with the increased rate, ascribed from the incomplete intercalation/de-intercalation of lithium-ions at high rate. Similar with the cyclic performance, the decay of rate capacity for the GPEs with nanoparticles is significantly lower than that of GPE without nanoparticles. The specific discharge capacities of GPE with 3.0 wt.% Al_2O_3 under the rate of 0.3*C* and 7*C* are 189.4 mAh g^{-1} in the 5th cycle and 123.2 mAh g^{-1} in the 25th cycle, which maintain 65% of that at 0.3*C* rate in 7*C* rate. Correspondingly, the rate capacity retention ability under 7*C* rate for GPE without nanoparticles is 62% of that at 0.3*C* (113.0 mAh g^{-1}@7*C* vs. 179.8 mAh g^{-1}@0.3*C*). To further understand its reversibility, the coin cells are cycled under 1*C* subsequently after high rate of 7*C*. It can be found from Fig. 7 that the discharge capacity is restored to 164.9 mAh g^{-1} for the GPE with 3.0 wt.% Al_2O_3, while is returned to only 146.3 mAh g^{-1} for the GPE without Al_2O_3 in the 30th cycle, suggesting that the doped GPE owns excellent rate performance.

As indicated from SEM image in Fig. 1, doping nanoparticles do improve the structure of the ceramic fiber membrane. Uniform fiber structure and smooth lithium ion migration channels after gelation make GPE have higher ionic conductivity, resulting in the enhancement in the rate performance. Furthermore, the superior interfacial compatibility between GPE and lithium anode reduces the transfer resistance in the bulk phase of GPE, which is beneficial to the charge transfer and interface conductivity of the electrode. Therefore, the amount of de-intercalation lithium ions in cathode material under high voltage conditions is increased, making the capacity utilize fully in the assembled battery under high voltage conditions.

Conclusions

Addition the nanoparticles into membrane does not affect the arrangement of polymer fibers although its morphology is changed to a certain extent. However, the proportion of nanoparticles affects the embedding amount on the surface of fiber membrane, which determines the difference between the specific surface area and porosity. The highest ionic conductivity at room temperature is 1.6×10^{-3} S cm^{-1} and the fracture stress is 177.1 MPa for the membrane doped with 3.0 wt.% Al_2O_3, ascribed from the membrane fully infiltrated by the liquid electrolyte can reduce the migration barrier of lithium ions in the bulk phase. Due to the good compatibility between the doped GPE and the electrode, the full cell composed of NCA/GPE/Li exhibits highest initial discharge capacity (174.5 mAh g^{-1}) and good cycle stability (89.4% @ 150 cycles) under high voltage condition. Thus, the facile tactics by doping a small amount of nanoparticle into the fiber membrane gives a bright future to develop high-energy-density lithium-ion batteries.

Acknowledgements The authors are highly grateful for the financial support from Guangdong Basic and Applied Basic Research Foundation (Grant No. 2021A1515010141) and Guangzhou Science and Technology Plan Project (Grant No. 202102080610).

References

1. Vishwakarma V, Jain A (2017) Enhancement of thermal transport in gel polymer electrolytes with embedded BN/Al_2O_3 nano− and micro−particles. J Power Sources 362:219–227
2. Zhao HJ, Deng NP, Ju JG, Li ZJ, Kang WM, Cheng BW (2019) Novel configuration of heat−resistant gel polymer electrolyte with electrospun poly (vinylidene fluoride−co−hexafluoropropylene) and poly−m−phenyleneisophthalamide composite separator for high−safety lithium−ion battery. Mater Lett 236:101–105
3. Luo L, Wang D, Zhou Z, Dong P, Yang S, Duan J, Zhang Y (2021) Engineering a robust interface on Ni−rich cathodes via a novel dry doping process toward advanced high−voltage performance. ACS Appl Mater Interfaces 13:45068–45076
4. Xu D, Jin J, Chen CH, Wen ZY (2018) From nature to energy storage: A novel sustainable 3D crosslinked chitosan−PEGGE based gel polymer electrolyte with excellent lithium ion transport properties for lithium batteries. ACS Appl Mater Interfaces 10:38526–38537
5. Unge M, Gudla H, Zhang C, Brandell D (2020) Electronic conductivity of polymer electrolytes: electronic charge transport properties of LiTFSI−doped PEO. Phys Chem Chem Phys 22:7680–7684
6. Jiang TL, He PG, Wang GX, Shen Y, Nan CW, Fan LZ (2020) Solvent−free synthesis of thin, flexible, nonflammable garnet−based composite solid electrolyte for all−solid−state lithium batteries. Adv Energy Mater 12:1903376
7. Li S, Zhang SQ, Shen L, Liu Q, Ma JB, Lv W, He YB, Yang QH (2020) Progress and perspective of ceramic/polymer composite solid electrolytes for lithium batteries. Adv Sci 5:1903088
8. Huang YX, Huang Y, Liu B, Cao HJ, Zhao L, Song AM, Lin YH, Wang MS, Li X, Zhang ZP (2018) Gel polymer electrolyte based on p(acrylonitrile−maleic anhydride) for lithium ion battery. Electrochim Acta 286:242–251
9. Wu N, Cao Q, Wang X, Li S, Li X, Deng H (2011) In situ ceramic fillers of electrospun thermoplastic polyurethane/poly (vinylidene fluoride) based gel polymer electrolytes for Li−ion batteries. J Power Sources 196:9751–9756
10. Li W, Xing Y, Wu Y, Wang J, Chen L, Yang G, Tang B (2015) Study the effect of ion−complex on the properties of composite gel polymer electrolyte based on electrospun PVdF nanofibrous membrane. Electrochim Acta 151:289–296

11. Liang SS, Yan WQ, Wu X, Zhang Y, Zhu YS, Wang HW, Wu YP (2018) Gel polymer electrolytes for lithium ion batteries: fabrication, characterization and performance. Solid State Ionics 318:2–18
12. Fenton DE, Parker JM, Wright PV (1973) Complexes of alkali metal ions with poly(ethylene oxide). Polymer 14:589
13. Zhu YS, Xiao SY, Li MX, Chang Z, Wang FX, Gao J, Wu YP (2015) Natural macromolecule based carboxymethyl cellulose as a gel polymer electrolyte with adjustable porosity for lithium ion batteries. J Power Sources 288:368–375
14. Zhu Y, Wang F, Liu L, Xiao S, Chang Z, Wu Y (2013) Composite of a nonwoven fabric with poly (vinylidene fluoride) as a gel membrane of high safety for lithium ion battery, Energ Environ Sci 6:618–624
15. Raghavan P, Manuel J, Zhao X, Kim DS, Ahn JH, Nah C (2011) Preparation and electrochemical characterization of gel polymer electrolyte based on electrospun polyacrylonitrile nonwoven membranes for lithium batteries. J Power Sources 196:6742–6749
16. Choi SW, Jo SM, Lee WS, Kim YR (2003) An electrospun poly (vinylidene fluoride) nanofibrous membrane and its battery applications. Adv Mater 15:2027–2032
17. Liao YH, Zhou DY, Rao MM, Li WS, Cai ZP, Liang Y, Tan CL (2009) Self−supported poly(methyl methacrylate−acrylonitrile−vinyl acetate)−based gel electrolyte for lithium ion battery. J Power Sources 189:139–144
18. Liang YF, Xia Y, Zhang SZ, Wang XL, Xia XH, Gu CD, Wu JB, Tu JP (2019) A preeminent gel blending polymer electrolyte of poly(vinylidene fluoride−hexafluoropropylene) −poly(propylene carbonate) for solid−state lithium ion batteries. Electrochim Acta 296:1064–1069
19. Seidel SM, Jeschke S, Vettikuzha P, Wiemhöfer HD (2015) PVDF−HFP/ether−modified polysiloxane membranes obtained via airbrush spraying as active separators for application in lithium ion batteries. Chem Commun 51:12048–12051
20. Zhang P, Yang LC, Li LL, Ding ML, Wu YP, Holze R (2011) Enhanced electrochemical and mechanical properties of P(VDF−HFP)−based composite polymer electrolytes with SiO_2 nanowires. J Membrane Sci 379:80–85
21. Dong YQ, Wang M, Chen L, Li MJ (2012) Preparation, characterization of P (VDF−HFP)/[bmim] BF_4 ionic liquids hybrid membranes and their pervaporation performance for ethyl acetate recovery from water. Desalination 295:53–60
22. Li M, Liao Y, Liu Q, Xu J, Chen F, Huang J, Li W (2018) Application of poly(vinylidene fluoride−co−hexafluoropropylene) blended poly(methyl vinyl ether−alt−maleic anhydride) based gel polymer electrolyte by electrospinning in Li−ion batteries. Solid State Ionics 325:57–66
23. Shi C, Dai J, Shen X, Peng L, Li C, Wang X, Zhang P, Zhao J (2016) A high−temperature stable ceramic−coated separator prepared with polyimide binder/Al_2O_3 particles for lithium−ion batteries. J Membrane Sci 517:91–99
24 Vijayakumar G, Karthick SN, SathiyaPriya AR, Ramalingam S, Subramania A (2008) Effect of nanoscale CeO_2 on PVDF−HFP−based nanocomposite porous polymer electrolytes for Li−ion batteries. J. Solid State Electrochem 12:1135–1141
25. Mishra K, Arif T, Kumar R, Kumar D, Subramania A (2019) Effect of Al_2O_3 nanoparticles on ionic conductivity of PVdF-HFP/PMMA blend-based Na^+-ion conducting nanocomposite gel polymer electrolyte. J Solid State Electrochem 23:2401–2409
26. Gu L, Zhang M, He J, Ni P (2018) A porous cross-linked gel polymer electrolyte separator for lithium-ion batteries prepared by using zinc oxide nanoparticle as a foaming agent and filler. Electrochim Acta 292:769–7781
27. Li W, Li X, Yuan A, Xie X, Xia B (2016) Al_2O_3/poly(ethylene terephthalate) composite separator for high-safety lithium-ion batteries. Ionics 22:2143–2149
28. Cheng J, Cao X, Zhou D, Tong Y (2020) Preparation of SiO_2 grafted polyimidazole solid electrolyte for lithium-ion batteries. Ionics 26:3883–3892
29. Xia Y, Li Y, Xiao Z, Zhou X, Wang G, Zhang J, Gan Y, Huang H, Liang C, Zhang W (2020) β-Cyclodextrin-modified porous ceramic membrane with enhanced ionic conductivity and thermal stability for lithium-ion batteries. Ionics 26:173–182
30. Huang W, Liao Y, Li G, He Z, Luo X, Li W (2017) Investigation on polyethylene supported poly(butyl methacrylate−acrylonitrile−styrene) terpolymer based gel electrolyte reinforced by doping nano−SiO_2 for high voltage lithium ion battery. Electrochim Acta 251:145–154
31. Liao Y, Chen T, Luo X, Fu Z, Li X, Li W (2016) Cycling performance improvement of polypropylene supported poly(vinylidene fluoride−co−hexafluoropropylene)/maleic anhydride−grated−polyvinylidene fluoride based gel electrolyte by incorporating nano−$Al_2O_3$for full batteries. J Membrane Sci 507:126–134
32. Sun P, Liao Y, Luo X, Li Z, Chen T, Xing L, Li W (2015) The improved effect of co−doping with nano−SiO_2 and nano−Al_2O_3 on the performance of poly(methyl methacrylate−acrylonitrile−ethyl acrylate) based gel polymer electrolyte for lithium ion batteries. RSC Adv 5:64368–64377
33. Liao YH, Li XP, Fu CH, Xu R, Zhou L, Tan CL, Hu SJ, Li WS (2011) Polypropylene–supported and nano–Al_2O_3 doped poly(ethylene oxide)–poly(vinylidene fluoride–hexafluoropropylene)–based gel electrolyte for lithium ion batteries. J Power Sources 196:2115–2121
34. Liao YH, Li WS (2017) Research progresses on gel polymer separators for lithium−ion batteries. Acta Phys Chim Sin 33:1533–1547
35. Liao YH, Rao MM, Li WS, Yang LT, Zhu BK, Xu R, Fu CH (2010) Fumed silica–doped poly(butyl methacrylate–styrene)–based gel polymer electrolyte for lithium ion battery. J Membrane Sci 352:95–99
36. Liao YH, Li XP, Fu CH, Xu R, Rao MM, Zhou L, Hu SJ, Li WS (2011) Performance improvement of polyethylene−supported poly(methyl methacrylate−vinyl acetate)−*co*−poly(ethylene glycol) diacrylate based gel polymer electrolyte by doping nano−Al_2O_3. J Power Sources 196:6723–6728
37. Li M, Liao Y, Liu Q, Xu J, Sun P, Shi H, Li W (2018) Application of the imidazolium ionic liquid based nano−particle decorated gel polymer electrolyte for high safety lithium ion battery. Electrochim Acta 284:188–201
38. Choktaweesap N, Arayanarakul K, Aht-Ong D, Meechaisue C, Supaphol P (2007) Electrospun gelatin fibers: effect of solvent system on morphology and fiber diameters. Polym J 39:622–631
39. Liao Y, Rao M, Li W, Tan C, Yi J, Chen L (2009) Improvement in ionic conductivity of self–supported P(MMA–AN–VAc) gel electrolyte by fumed silica for lithium ion batteries. Electrochim Acta 54:6396–6402
40. Bruce PG, Vincent CA (1987) Steady state current flow in solid binary electrolyte cells. J Electroanal Chem 225:1–17
41. Christie L, Christie AM, Vincent CA (1999) Measurement of the apparent lithium ion transference number and salt diffusion coefficient in solid polymer electrolytes. Electrochim Acta 44:2909–2913
42. Li Z, Su G, Gao D, Wang X, Li X (2004) Effect of Al_2O_3 nanoparticles on the electrochemical characteristics of P(VdF−HFP)−based polymer electrolyte. Electrochim Acta 49:4633–4639